

Azimuthal dependence of pion source radii in Pb+Au collisions at 158A GeV/c

D. Adamová,¹ G. Agakichiev,² A. Andronic,³ D. Antończyk,⁴ H. Appelshäuser,⁴ V. Belaga,² J. Bielčíková,^{5,6} P. Braun-Munzinger,³ O. Busch,⁶ A. Cherlin,⁷ S. Damjanović,⁶ T. Dietel,⁸ L. Dietrich,⁶ A. Drees,⁹ W. Dubitzky,⁶ S. I. Esumi,⁶ K. Filimonov,⁶ K. Fomenko,² Z. Fraenkel,^{7,*} C. Garabatos,³ P. Glässel,⁶ G. Hering,³ J. Holeczek,³ M. Kalisky,⁸ S. Kniege,⁴ V. Kuschpil,¹ A. Maas,³ A. Marín,³ J. Milošević,⁶ D. Miśkowiec,³ R. Ortega,⁶ Y. Panebrattsev,² O. Petchenova,² V. Petráček,⁶ M. Płoskoń,⁴ S. Radoski,⁶ J. Rak,³ I. Ravinovich,⁷ P. Rehak,¹⁰ H. Sako,³ W. Schmitz,⁶ S. Schuchmann,⁴ J. Schukraft,¹¹ S. Sedykh,³ S. Shimansky,² R. Soualah,⁶ J. Stachel,⁶ M. Šumbera,¹ H. Tilsner,⁶ I. Tserruya,⁷ G. Tsileadakis,³ J. P. Wessels,⁸ T. Wienold,⁶ J. P. Wurm,⁵ S. Yurevich,³ and V. Yurevich²

¹Nuclear Physics Institute of ASCR, 25068 Řež, Czech Republic

²Joint Institute for Nuclear Research, RU-141980 Dubna, Russia

³GSI Helmholtzzentrum für Schwerionenforschung GmbH, D-64291 Darmstadt, Germany

⁴Institut für Kernphysik der Goethe-Universität, D-60438 Frankfurt am Main, Germany

⁵Max Planck Institute for Nuclear Physics, D-69117 Heidelberg, Germany

⁶Physikalisches Institut of the University of Heidelberg, D-69120 Heidelberg, Germany

⁷Weizmann Institute of Science, Rehovot 76100, Israel

⁸University of Münster, D-48149 Münster, Germany

⁹Stony Brook University, Stony Brook, NY 11794, USA

¹⁰Brookhaven National Lab, Upton, NY 11973, USA

¹¹European Organization for Nuclear Research CERN, 1211 Geneva, Switzerland

(Received 16 May 2008; published 4 December 2008)

We present results of a two-pion correlation analysis performed with the Pb+Au collision data collected by the upgraded CERES experiment in the fall of 2000. The analysis was done in bins of the reaction centrality and the pion azimuthal emission angle with respect to the reaction plane. The pion source, deduced from the data, is slightly elongated in the direction perpendicular to the reaction plane, similarly as was observed at the Brookhaven National Laboratory Alternating Gradient Synchrotron and Relativistic Heavy Ion Collider.

DOI: 10.1103/PhysRevC.78.064901

PACS number(s): 25.75.Gz, 25.75.Ld

I. INTRODUCTION

Two-particle correlations provide unique access to the spatial extension of the source of particles emitted in the course of heavy-ion collisions at relativistic energy (for a recent review see Ref. [1]). The relation between the experimental correlation function, defined as the relative momentum distribution of pairs, normalized to the analogous distribution obtained via event mixing, and the size of the fireball is especially simple in case of identical pions where the main source of correlations is the Bose-Einstein statistics. In fact, in the pure boson case the correlation function is

$$C(\mathbf{q}, \mathbf{P}) = 1 + \frac{|\int d^4x S(x, P) \exp(iq \cdot x)|^2}{|\int d^4x S(x, P)|^2}, \quad (1)$$

with the source function $S(x, P)$ describing the single-particle density in eight-dimensional position-momentum space at freeze-out. The correlation function C depends on the momentum difference $\mathbf{q} = \mathbf{p}_2 - \mathbf{p}_1$ and the mean pion momentum $\mathbf{k} = (\mathbf{p}_1 + \mathbf{p}_2)/2$. The width of the peak at $\mathbf{q} = 0$ is inversely proportional to the source radius. A particularly exciting prospect is to look for a source asymmetry possibly reflecting the initial asymmetry of the fireball created in collisions with finite impact parameter [2–5]. Indeed, significant dependence of the source radii on the azimuthal emission angle with

respect to the reaction plane, defined by the beam axis and the impact parameter vector, was observed in Au+Au collisions at 2–6 GeV [6] and at $\sqrt{s} = 200$ GeV [7]. In this article we present results of the first analysis of the azimuthal dependence of pion source radii at SPS energies.

II. EXPERIMENT

The CERES/NA45 experiment at the CERN Super Proton Synchrotron (SPS) is described in detail in Ref. [8]. The upgrade by a radial Time Projection Chamber (TPC) in 1997–1998, in addition to improving the dilepton mass resolution, enhanced the experiment's capability of studying hadronic observables. The cylindrical symmetry of the experiment was preserved during the upgrade, making the setup ideally suited to address azimuthal anisotropies. About 30 million Pb+Au collision events at 158A GeV/c were collected in the fall of 2000, most of them with centrality within the top 7% of the geometrical cross section σ_G . Small samples of $\sigma/\sigma_G = 20\%$ and minimum bias collisions, as well as a short run at 80A GeV, were recorded in addition.

III. DATA ANALYSIS

The results presented here are based on a correlation analysis of the high-statistics Pb+Au data set from the year

*Deceased.

2000 [9]. The results of an azimuthal-angle averaged analysis in Ref. [9] are consistent with the previously published CERES data [10] and with a recent analysis by the NA49 Collaboration [11]. The main steps of the azimuthal-angle-dependent analysis are described below.

A. Event selection

The collision centrality was determined via the charged particle multiplicity around midrapidity $y_{\text{beam}}/2 = 2.91$. Two variables, the amplitude of the multiplicity counter (MC) (single scintillator covering $2.3 < \eta < 3.5$) and the track multiplicity in the TPC ($2.1 < \eta < 2.8$), were alternatively used as the centrality measure. Knowing the data acquisition dead time factor and the target thickness, and assuming that all beam particles were hitting the target, the event counts were translated to the cross section for collisions with a given multiplicity. The centrality variable used in this paper is defined as the integrated cross section divided by the geometrical cross section $\sigma_G = 6.94$ barn.

The fireball created in a collision with finite impact parameter is elongated in the direction perpendicular to the reaction plane. In the course of expansion, with the pressure gradient larger in-plane than out-of-plane, the initial asymmetry should get reduced or even reversed. Experimentally, the source eccentricity at the time of decoupling can be determined from an analysis of two-pion correlations as function of $\Phi^* = \Phi_{\text{pair}} - \Psi_{\text{RP}}$, the pair emission angle with respect to the reaction plane.

The azimuthal angle of the reaction plane Ψ_{RP} was estimated by the preferred direction of the particle emission (elliptic flow). For this, in each event the flow vector \mathbf{Q}_2 was constructed out of the measured particles, characterized by transverse momenta p_t and azimuthal emission angles ϕ [12,13]:

$$Q_2^X = \frac{1}{N} \sum_{i=1}^N p_{t,i} \cos(2\phi_i) \quad (2)$$

$$Q_2^Y = \frac{1}{N} \sum_{i=1}^N p_{t,i} \sin(2\phi_i). \quad (3)$$

The Q_2^X and Q_2^Y components were calibrated (shifted and scaled) such that the peak in the (Q_2^X, Q_2^Y) distribution was centered at (0,0), and its widths in the directions of X and Y were equal. The reaction plane angle was calculated (modulo π) from the calibrated \mathbf{Q}_2 via

$$\Psi_{\text{RP}} = \frac{1}{2} \arctan \frac{Q_2^Y}{Q_2^X}. \quad (4)$$

The resolution of the so determined reaction plane angle, estimated via the subevent method [12,14], was 30–34°.

The event mixing, needed to obtain the denominator of the correlation functions, was performed in bins of centrality (2% of σ_G), event plane (15°), and vertex (same target disk). This ensures that the shape of the background is identical to that of the signal in all respects except for the femtoscopic correlations.

B. Track selection

Only TPC tracks with at least 12 (of maximally 20) hits and a reasonably good χ^2 , falling into the fiducial acceptance $0.125 < \theta < 0.240$, were used in the analysis. A momentum-dependent dE/dx cut was applied to reduce the contamination of the pion sample. Pions from K^0 and Λ^0 decays were suppressed by a 2.5σ matching cut between the silicon vertex detectors and the TPC.

C. Pair selection

The two-track resolution cuts applied to the true pairs and to the pairs from event mixing were different for the two possible track pair topologies: in the case of the magnetic field bringing the tracks apart from each other (sailor) the required two-track separation was $\Delta\phi > 38\text{--}45$ mrad, depending on the transverse momentum; for the opposite (cowboy) case, $\Delta\phi > 90\text{--}140$ mrad was used. The polar angle cut was the same for both topologies ($\Delta\theta > 8\text{--}9$ mrad). It should be noted that the required two-track cuts depended somewhat on the quality cuts applied to single tracks: the higher the number of hits required for single tracks, the more pairs were lost because of the finite two-track resolution.

D. Correlation functions

The two-pion analysis was performed in the longitudinally comoving frame (LCMS) defined by the vanishing z component of the pair momentum. The momentum difference in this frame, $\mathbf{q} = \mathbf{p}_2 - \mathbf{p}_1$, was decomposed into the “out,” “side,” and “long” components following the Bertsch-Pratt convention, with q_{out} pointing along the pair transverse momentum and q_{long} along the beam [15]. The two particles were numbered such that q_{side} was always positive.

The $\pi^-\pi^-$ and $\pi^+\pi^+$ correlation functions were fitted by

$$C_2(\mathbf{q}) = N \cdot \{(1 - \lambda) + \lambda \cdot F_c(\mathbf{q})[1 + G(\mathbf{q})]\},$$

$$G(\mathbf{q}) = \exp\left(-\sum_{i,j} R_{ij}^2 q_i q_j\right) \quad (5)$$

with the indices $i, j = \{\text{out, side, long}\}$ [16]. An example of the fit is shown in Fig. 1. The normalization factor N was needed because the number of pairs from event mixing was four times higher than that of signal pairs. The correlation strength $\lambda < 1$ reflects the contribution of pions from long-lived resonances, the contamination of the pion sample by other particle species, and the finite \mathbf{q} resolution. The resulting source radii $\sqrt{R_{ij}^2}$ describe the size of the source emitting pions of a given momentum [1]. The $F_c(q_{\text{inv}})$ factor, $q_{\text{inv}} = \sqrt{-(p_2^\mu - p_1^\mu)^2}$, accounts for the mutual Coulomb interaction between the pions and was calculated by averaging the nonrelativistic Coulomb wave function squared over a realistic source size. The Coulomb factor was attenuated by λ similarly as the rest of the correlation function peak; the importance of this approach was demonstrated in Ref. [10]. The fits were performed by the minimum negative log-likelihood method, assuming that the number of true pairs in a given bin is

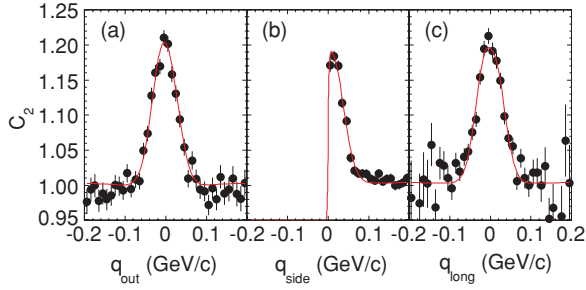


FIG. 1. (Color online) Example of the fit to a three-dimensional correlation function ($\pi^- \pi^-$, centrality 15–25%, one of the eight bins of the azimuthal pair angle with respect to the reaction plane). Shown are the projections of the correlation function on q_{out} , q_{side} , and q_{long} (a, b, and c, respectively) performed requiring the other two coordinates to be within $(-40 \text{ MeV}/c, 40 \text{ MeV}/c)$ (full dots). The analogous projections of the three-dimensional fit function (5) are shown as a solid red line. See footnote [16].

distributed around the expected mean value (equal to the number of mixed pairs times the fit function) according to the Poisson statistics. The source radii obtained from the fit were corrected for the finite momentum resolution

$$\frac{\Delta p}{p} = 2\% \oplus 1\% \cdot p/(\text{GeV}/c). \quad (6)$$

The correction was determined by Monte Carlo and is rather insignificant for R_{side} and R_{long} ; for R_{out} it gets as large as $\approx +20\%$ for the highest pion momenta.

E. Azimuthal dependence of pion source radii

Correlation functions were generated separately for pion pairs with different azimuthal angles with respect to the reaction plane $\Phi^* = \Phi_{\text{pair}} - \Psi_{\text{RP}}$. For this, the pions were sorted into eight bins covering $(-\pi/2, \pi/2)$. The eight correlation functions were fitted as described in Sec. III D [16] and the resulting squared source radii were parametrized by [17]

$$\begin{aligned} R_{\text{out}}^2 &= R_{\text{out},0}^2 + 2R_{\text{out},2}^2 \cos(2\Phi^*) \\ R_{\text{side}}^2 &= R_{\text{side},0}^2 + 2R_{\text{side},2}^2 \cos(2\Phi^*) \\ R_{\text{long}}^2 &= R_{\text{long},0}^2 + 2R_{\text{long},2}^2 \cos(2\Phi^*) \\ R_{\text{os}}^2 &= 2R_{\text{os},2}^2 \sin(2\Phi^*) \\ R_{\text{ol}}^2 &= R_{\text{ol},0}^2 + 2R_{\text{ol},1}^2 \cos(\Phi^*) \\ R_{\text{sl}}^2 &= 2R_{\text{sl},1}^2 \sin(\Phi^*). \end{aligned} \quad (7)$$

This step of analysis is illustrated in Fig. 2. While the $R_{\text{out},0}^2$, $R_{\text{side},0}^2$, and $R_{\text{long},0}^2$ obtained represent the ϕ -averaged squared pion HBT radii, the second Fourier coefficients $R_{i,2}^2$ describe the eccentricity of the observed pion source. Because the reaction plane is known modulo π odd Fourier components should vanish. If the pion source were to reflect the initial collision geometry (almond shape out-of-plane) a positive $R_{\text{side},2}^2$ and $R_{\text{os},2}^2$ and a negative $R_{\text{out},2}^2$ should be expected. For symmetry reasons all anisotropies should disappear in the limit of central collisions.

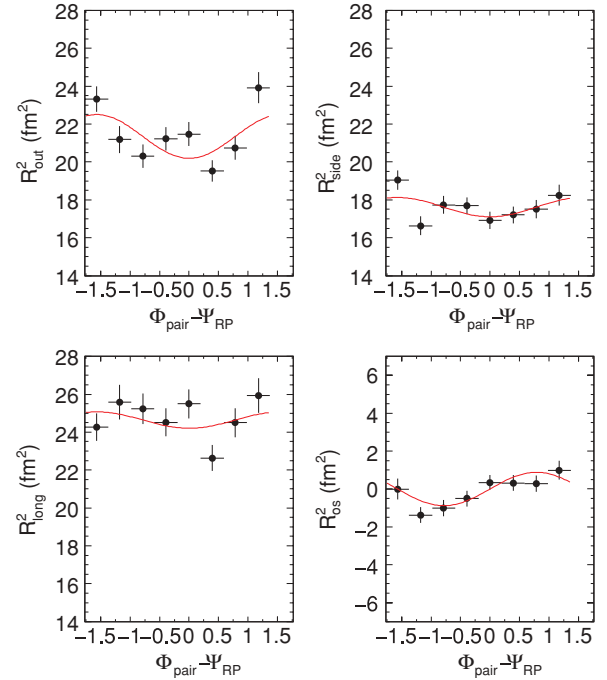


FIG. 2. (Color online) Example of the azimuthal angle dependence of the squared source radii (centrality 15–25%, combined positive and negative pions) (full dots) and the fit by Eq. (7) (red line). The purpose of this figure is to illustrate the analysis principle and to give an impression of the statistical errors; the actual analysis was performed in bins of pair transverse momentum [16].

The second Fourier coefficients $R_{i,2}^2$ have been corrected for the reaction plane resolution by dividing them by the mean cosine of twice the difference between the reconstructed and the true reaction plane angles $\langle \cos[2(\Psi_{\text{RP}}^{\text{rec}} - \Psi_{\text{RP}})] \rangle$, estimated via the measured mean cosine of the difference between two subevents:

$$R_{i,2}^2 \rightarrow \frac{R_{i,2}^2}{\sqrt{2\langle \cos[2(\Psi_b - \Psi_a)] \rangle}}, \quad (8)$$

similarly as it is done for flow measurements [14]. The correction factor was between 4.8 and 2.4 (centralities of 0–2.5% and 25–70%, respectively). It has been pointed out in [17] that the correct way to introduce the finite reaction plane resolution is by calculating its impact on the pair distributions. The appropriateness of the simple flow-like correction described above for our two-pion correlation data was verified with a Monte Carlo simulation of pion pairs emitted from an elliptical source; the observed reduction of the second Fourier coefficients of squared radii was, within the statistical errors of the simulation (about 10%), in agreement with Eq. (8).

F. Systematic errors

The fact that separate analyses of positive and negative pions give consistent results indicates that the limited particle identification is not causing any bias. The systematic error related to the reaction plane resolution correction, based on

the comparison between Eq. (8) and a numerical simulation, is estimated to be not larger than 10%. Autocorrelations, i.e., using the same particles to determine the event plane and the HBT radii, might be another source of systematic errors; unfortunately, an attempt to exclude the two particles from the event plane construction led to a strong distortion of the correlation functions as it was not clear how to do the exclusion consistently for the true and mixed pairs. An independent way to estimate the overall systematic errors is by inspecting (see Fig. 3 in the next section) the coefficients $R_{ol,1}^2$ and $R_{sl,1}^2$ which should be zero because the reaction plane is known only modulo π . Averaged over centralities, they are 0.40 ± 0.16 and 0.22 ± 0.06 fm², respectively. Attributing part (one σ) of the deviation to statistical fluctuation we are left with a discrepancy of about 0.3 fm² that we thus assume to be the systematic uncertainty of the results presented.

IV. RESULTS AND DISCUSSION

The extracted Fourier coefficients are shown in Table I and Fig. 3 [18]. The anisotropies in the out and side directions indicate a pion source elongated out-of-plane. For comparison, the Brookhaven National Laboratory Alternating Gradient Synchrotron (AGS) [6] and Relativistic Heavy Ion Collider (RHIC) [7,19] values, obtained by performing the fits using Eq. (7) on their published radii (the AGS results were subsequently corrected for their reaction plane resolution), are represented in Fig. 3 by open symbols and stars.

The fact that the magnitude of the R_{side} anisotropy seems to be weaker than that of R_{out} indicates that not only the source geometry but also azimuthal dependence of the emission time might play a role. However, $R_{out,2}^2 - R_{side,2}^2 + 2R_{os,2}^2$, averaged over centralities, is 0.06 ± 0.18 fm², consistent with zero. This implies that the sum rule from Ref. [17], which is supposed to be valid for systems with emission time independent on the azimuthal angle, works rather well.

The R_{long} anisotropy is negative and roughly independent of centrality. A series of checks were performed to make sure that this is not an artifact of the analysis. This result might indicate that R_{long} is sensitive to fluctuations of the azimuthal particle density. A hydrodynamical calculation performed for noncentral collisions at RHIC energies [20] (see also Fig. 25 in Ref. [21]) yields an $R_{long,2}^2$ of about -1 fm², i.e., comparable to our data. An analogous calculation [22] of Pb+Au collisions at our energy and centrality also yields a similar amount of anisotropy

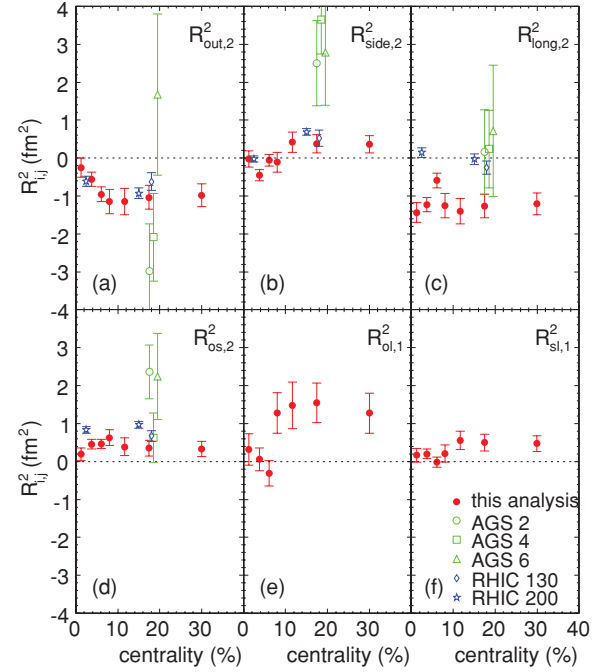


FIG. 3. (Color online) Azimuthal pion source eccentricity, represented by the second Fourier coefficient of the azimuthal angle dependence of R_{out}^2 , R_{side}^2 , R_{long}^2 , R_{os}^2 (a–d), measured in Pb+Au collisions as a function of centrality. Fourier coefficients of positive and negative pions have been combined. The mean pion transverse momentum is 0.23 GeV/c. For comparison, analogous measurements at the AGS (open green symbols) and RHIC (blue diamonds and stars for 130 and 200 GeV, respectively) are shown. The first Fourier coefficients $R_{ol,1}^2$ and $R_{sl,1}^2$ (e and f) should be zero by construction. The estimated systematic error is 0.3 fm².

in R_{long}^2 which, however, disappears in the limit of zero impact parameter [22]. The blast-wave model with parameters adjusted to RHIC data yields a nearly centrality independent $R_{long,2}^2/R_{long,0}^2$ and attributes it to the elliptic flow [21]. The magnitude of this oscillation, however, is about one-tenth of the one we observe. All this indicates that the knowledge about the mechanism leading to oscillations of R_{long} is still incomplete.

The source radius anisotropies for centrality 15–25% are shown as a function of the collision energy in Fig. 4. The geometrical pion source eccentricity, which can be quantified via $\varepsilon \approx 2R_{side,2}^2/R_{side,0}^2$, has at the SPS a value of 0.043 ± 0.027 ,

TABLE I. Fourier coefficients from a fit of Eq. (7) to the pion source radii squared. The values are in fm².

Centrality	Mean cent.	$R_{out,0}^2$	$R_{side,0}^2$	$R_{long,0}^2$	$R_{ol,0}^2$	$R_{out,2}^2$	$R_{side,2}^2$	$R_{long,2}^2$	$R_{os,2}^2$
0–2.5%	1.3%	29.34(10)	24.33(08)	33.10(11)	−6.56(21)	−0.25(25)	−0.03(21)	−1.43(26)	0.19(17)
2.5–5%	3.7%	28.01(08)	23.29(06)	31.91(09)	−5.72(18)	−0.56(19)	−0.45(15)	−1.23(19)	0.45(13)
5–7.5%	6.1%	26.62(08)	22.04(06)	30.61(10)	−5.22(15)	−0.96(19)	−0.06(15)	−0.59(19)	0.46(12)
7.5–10%	8.1%	25.39(17)	21.00(13)	29.22(21)	−5.20(31)	−1.15(32)	−0.11(26)	−1.25(32)	0.63(21)
10–15%	11.6%	23.83(19)	19.87(14)	27.31(23)	−4.33(37)	−1.14(35)	0.42(27)	−1.40(34)	0.39(23)
15–25%	17.5%	21.35(23)	17.62(17)	24.64(28)	−3.67(48)	−1.03(31)	0.38(24)	−1.27(30)	0.35(21)
25–70%	30.0%	14.28(49)	12.29(35)	17.42(61)	−4.23(116)	−0.98(30)	0.36(23)	−1.20(29)	0.34(20)

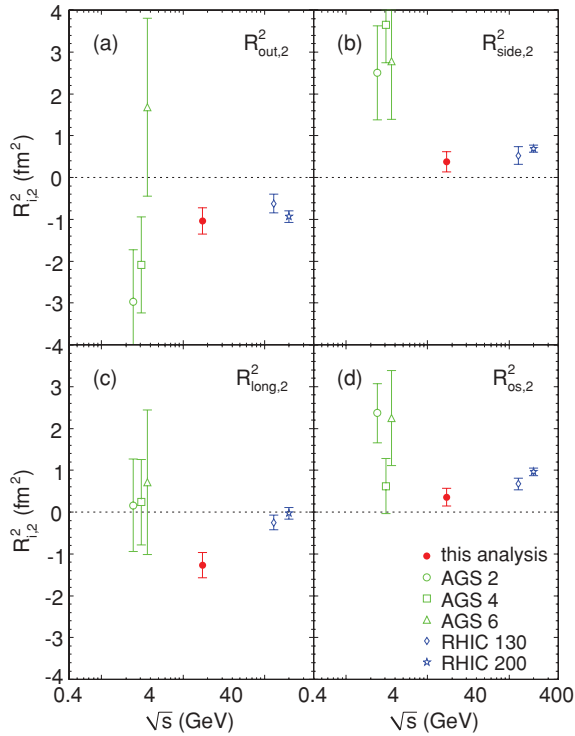


FIG. 4. (Color online) Collision energy dependence of the pion source out, side, long, and out-side anisotropies (a–d, respectively) in Au+Au and Pb+Au collisions at the 15–25% centrality. The meaning of the symbols is the same as in Fig. 3. The SPS anisotropies are rather similar to those obtained at RHIC, except for the R_{long} one (c) that is significantly off-zero. The estimated systematic error is 0.3 fm^2 .

significantly less than the initial fireball eccentricity at this collision centrality $\varepsilon_{\text{initial}} \approx 0.20$ [7]. It is also much lower than at AGS (0.25 ± 0.05) and somewhat lower than RHIC (0.074 ± 0.010). Taken at face value this would mean that the pion source eccentricity behaves nonmonotonically with the collision energy. A nonmonotonic energy evolution of interferometric observables, in particular of the freeze-out volume, was reported earlier [23]. These observations were understood in the context of a constant mean free path at freeze-out; however, implications for source anisotropies in noncentral collisions have not yet been considered. The statistical significance of the SPS-RHIC difference, however, is on the one- σ level and thus the only statement one can make is that the eccentricity quickly drops between the AGS and SPS

and stays approximately constant up to the RHIC energies. In any case the data show no indication of a systematic trend that could result in a negative eccentricity (“in-plane extended source”) at the LHC, predicted in Refs. [20,24].

The $R_{\text{long},2}^2$ is about -1 fm^2 at the SPS and approaches zero at RHIC. This trend is similar to the one predicted by hydrodynamics [24] although there it is expected to happen between RHIC and LHC. Thus, both the transverse and longitudinal radius anisotropies at the SPS exhibit interesting behavior that makes the perspective of a systematic study in the course of the low-energy scan at RHIC particularly exciting, especially that with the statistical errors of the present AGS data even significant structures in the energy dependence of the pion source anisotropy cannot be excluded.

V. SUMMARY

We have analyzed the azimuthal angle dependence of the pion HBT radii in Pb+Au collisions at the top SPS energy. The source anisotropy in the out and side directions has the same sign and similar magnitude as the one measured at the AGS and at RHIC, and indicates a pion source elongated out-of-plane. The side anisotropy is somewhat smaller than the other which suggests that finite emission times may play a role. The source anisotropy in the long direction is negative for all centralities, indicating that R_{long} might be sensitive to particle density fluctuations.

ACKNOWLEDGMENTS

The CERES collaboration acknowledges the good performance of the CERN PS and SPS accelerators as well as the support from the EST division. We thank R. Campagnolo, L. Musa, A. Przybyla, W. Seipp, and B. Windelband for their contribution during construction and commissioning of the TPC and during data taking. We are grateful for excellent support by the CERN IT division for the central data recording and data processing. This work was supported by GSI, Darmstadt, the German BMBF, the HGF Virtual Institute 146 VI-SIM, the US Department of Energy, the Czech Science Foundation, the Israel Science Foundation, the Minerva Foundations, and the Nella and Leon Benozziyo Center for High Energy Physics Research.

- [1] M. A. Lisa, S. Pratt, R. Soltz, and U. Wiedemann, *Annu. Rev. Nucl. Part. Sci.* **55**, 357 (2005).
- [2] S. A. Voloshin and W. E. Cleland, *Phys. Rev. C* **53**, 896 (1996).
- [3] S. A. Voloshin and W. E. Cleland, *Phys. Rev. C* **54**, 3212 (1996).
- [4] U. A. Wiedemann, *Phys. Rev. C* **57**, 266 (1998).
- [5] M. A. Lisa, U. Heinz, and U. A. Wiedemann, *Phys. Lett.* **B489**, 287 (2000).
- [6] M. A. Lisa *et al.*, *Phys. Lett.* **B496**, 1 (2000).
- [7] J. Adams *et al.*, *Phys. Rev. Lett.* **93**, 012301 (2004).
- [8] A. Marín *et al.*, *J. Phys. G: Nucl. Part. Phys.* **30**, S709 (2004); D. Adamová *et al.*, *Nucl. Instr. Meth. A* **593**, 203 (2008).
- [9] D. Antończyk, Ph.D. thesis, Technical University Darmstadt, 2006.
- [10] D. Adamová *et al.*, *Nucl. Phys.* **A714**, 124 (2003).
- [11] S. Kniese, Ph.D. thesis, Frankfurt University 2005; C. Alt *et al.*, *Phys. Rev. C* **77**, 064908 (2008).
- [12] P. Danielewicz and G. Odyniec, *Phys. Lett.* **B157**, 146 (1985).
- [13] J. Barrette *et al.*, *Phys. Rev. Lett.* **73**, 2532 (1994); S. Voloshin and Y. Zhang, *Z. Phys. C* **70**, 665 (1996).

- [14] A. M. Poskanzer and S. A. Voloshin, Phys. Rev. C **58**, 1671 (1998).
- [15] G. F. Bertsch, Nucl. Phys. **A498**, 173c (1989); S. Pratt, Phys. Rev. D **33**, 1314 (1986).
- [16] To avoid possible problems caused by the non-Gaussian shape of inclusive correlation functions the fit to $R^2(\Phi^*)$ was actually performed in bins of pair k_T . The $R_{i,2}^2$'s discussed in this article are weighted averages of the $R_{i,2}^2$'s obtained for different k_T 's. The correlation functions presented in Figs. 1 and 2, however, are k_T -integrated ones such that the figures reflect the actual statistics, even if not necessarily the shape.
- [17] U. Heinz, A. Hummel, M. A. Lisa, and U. A. Wiedemann, Phys. Rev. C **66**, 044903 (2002).
- [18] We refrain in Fig. 3 from normalizing the coefficients to the corresponding mean source radii. In fact, since the second Fourier coefficients measured at RHIC [7] seem to be, within the measurement errors, independent of transverse momentum while the mean radii vary by about 40%, normalization to mean radii could wash out the weak oscillation we are after.
- [19] R. C. Wells, Ph.D. thesis, Ohio State University, 2002.
- [20] U. Heinz and P. F. Kolb, Phys. Lett. **B542**, 216 (2002).
- [21] F. Retière and M. A. Lisa, Phys. Rev. C **70**, 044907 (2004).
- [22] P. F. Kolb, P. Huovinen, U. W. Heinz, and H. Heiselberg, Phys. Lett. **B500**, 232 (2001); G. Agakichiev *et al.*, Phys. Rev. Lett. **92**, 032301 (2004); P. Huovinen (private communication).
- [23] D. Adamović *et al.*, Phys. Rev. Lett. **90**, 022301 (2003).
- [24] E. Frodermann, R. Chatterjee, and U. Heinz, J. Phys. G: Nucl. Part. Phys. **34**, 2249 (2007).